

## Research Article

# On Calculating the Packing Efficiency for Embedding Hexagonal and Dodecagonal Sensors in a Circular Container

Marina Prvan ,<sup>1</sup> Julije Ožegović ,<sup>1</sup> and Arijana Burazin Mišura ,<sup>2</sup>

<sup>1</sup>Faculty of Electrical Engineering, Mechanical Engineering and Naval Architecture (FESB), University of Split, Split 21000, Croatia

<sup>2</sup>University Department of Professional Studies, University of Split, Split 21000, Croatia

Correspondence should be addressed to Marina Prvan; [mprvan@fesb.hr](mailto:mprvan@fesb.hr)

Received 19 March 2019; Accepted 8 June 2019; Published 10 July 2019

Academic Editor: Vyacheslav Kalashnikov

Copyright © 2019 Marina Prvan et al. This is an open access article distributed under the Creative Commons Attribution License, which permits unrestricted use, distribution, and reproduction in any medium, provided the original work is properly cited.

In this paper, a problem of packing hexagonal and dodecagonal sensors in a circular container is considered. We concentrate on the sensor manufacturing application, where sensors need to be produced from a circular wafer with maximal silicon efficiency (SE) and minimal number of sensor cuts. Also, a specific application is considered when produced sensors need to cover the circular area of interest with the largest packing efficiency (PE). Even though packing problems are common in many fields of research, not many authors concentrate on packing polygons of known dimensions into a circular shape to optimize a certain objective. We revisit this problem by using some well-known formulations concerning regular hexagons. We provide mathematical expressions to formulate the difference in efficiency between regular and semiregular tessellations. It is well-known that semiregular tessellation will cause larger silicon waste, but it is important to formulate the ratio between the two, as it affects the sensor production cost. The reason why we have replaced the “perfect” regular tessellation with semiregular one is the need to provide spacings at the sensor vertices for placing mechanical apertures in the design of the new CMS detector. Archimedean  $\{3, 12^2\}$  semiregular tessellation and its more flexible variants with irregular dodecagons can provide these triangular spacings but with larger number of sensor cuts. Hence, we construct an irregular convex hexagon that is semiregularly tessellating the targeted area. It enables the sensor to remain symmetric and hexagonal in shape, even though irregular, and produced with minimal number of cuts with respect to dodecagons. Efficiency remains satisfactory, as we show that, by producing the proposed irregular hexagon sensors from the same wafer as a regular hexagon, we can obtain almost the same SE.

## 1. Introduction

Packing is a common problem in many different fields, such as computer science, design, manufacturing, and engineering. It consists of embedding smaller shapes into a larger one called container [1–4]. Basic requirements must be considered depending on the specific application to find the optimal packing efficiency (PE). For example, inner shapes can be the same in area or mixed shapes can be considered [5]. Also, arranged components can be nonoverlapping or there could be overlap allowed [6].

There are applications with different optimization goals, like minimizing the size of the container, or maximizing the number of arranged inner components [7, 8]. The shape of the container and the packed items may vary from a fixed-size circle, square, rectangle, triangle, etc. For example, circle

packing into a larger circle or a square is well addressed in the literature [9–13].

Packing problem can be mapped to the field of sensor manufacturing [14–16]. In this case, packing is a problem of producing  $N$  sensors from a circular silicon wafer which is a fixed-size container. The goal is to cut out as many sensors as possible from a given (in our case, circular) piece of silicon wafer material. Basic requirement is to minimize the silicon waste, i.e., the unused part of a circular object. PE is equated this way with the efficiency of the used silicon material or silicon efficiency (SE).

When producing a single sensor, it is known that SE is maximal if hexagon shape is used with respect to triangle or square [17, 18]. Since hexagon is the closest to being circular with the largest area, it has been shown to provide minimized silicon waste with respect to other geometrical shapes [19].

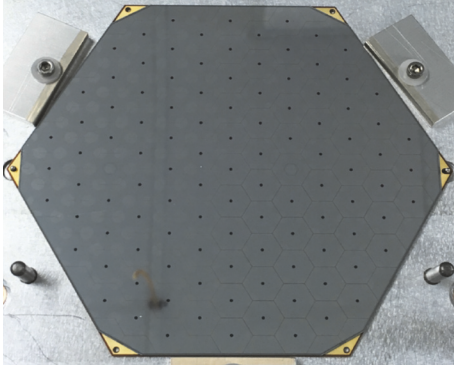


FIGURE 1: A hexagonal silicon sensor for CMS [30].

However, most papers in the literature concentrate only on producing rectangular or squared sensors. Namely, in the past, sensor dies were separated by the specific laser cutting procedure, applying only straight lines on the wafer in the manufacturing process [20, 21]. The former is known as “guillotine cutting” from one edge to the other [22]. Using the single straight lines is allowed with the regular pattern, so this mechanism forced dies to have regular shapes such as squares and rectangles.

Nowadays, it is possible to use methods of forming a semiconductor die that does not require applying only the single straight lines. Hence, dies having various nonrectangular shapes can be formed, increasing the wafer yield [23, 24]. Polygon dies further maximize the wafer utilization and multipolygon die packing may allow for a significant reduction of the wafer silicon material from which the polygon dies are produced [25].

Many applications require production and use of these abovementioned polygonal sensors, especially hexagons [26, 27]. One specific application in our focus is the design upgrade of the new CMS detector. For this purpose, hexagonal sensors are produced from six-inch or eight-inch wafer sizes. With these produced sensors, the aim is to efficiently cover a circular detector area of interest which is a circular container in the packing context [28, 29]. According to [1], the corners of the hexagons are flattened, providing a triangular gap wherever three hexagons meet. One regular hexagonal sensor for this purpose is shown in Figure 1 [30]. It has cut out triangles or “vertex cuts” needed to provide mechanical apertures when covering the detector surface.

With these vertex cuts, irregular dodecagon sensor shape needs to be produced, where a regular dodecagon is obtained with maximal cut applied. SE is expected to be larger when a single sensor is produced, but with 12 straight cuts applied on the wafer in the manufacturing process. The question that is posed in this study is can we construct a sensor whose geometrical shape can be as efficient in terms of minimal number of six cuts such as using a regular hexagon? Possibly, for these irregular hexagonal sensors, no vertex cuts are needed since they are provided by default in the tessellation process.

Naturally, applying the vertex cuts and using the irregular sensors both decrease SE when  $N$  sensors are produced, because semiregular tessellation is expected to cause larger silicon waste than regular tessellation. Nevertheless, the goal is to analyse whether using an irregular convex hexagon is cost-effective. We discuss if it is as efficient as using a regular hexagon. We also compare its efficiency with dodecagons, to see whether using the vertex cuts on tessellated regular hexagons is more efficient after all in terms of packing and production cost.

The paper is organized as follows. First, related work is summarized in Section 2 and the theoretical background on mathematical tessellation is given in Section 3. The used methodology of the research is explained in Section 4. Next, in Sections 5 and 6, packing regular and irregular polygons into a circular container is considered, and solutions to the defined problem statements are provided with the PE calculation formulas. An irregular convex hexagonal sensor shape is proposed in Section 6. Results are provided in Section 7, by comparing the packings. We give a real-life example where a concrete SE is calculated for six-inch or eight-inch wafers used. Section 8 concludes the paper together with the future work and it is followed by the references used.

## 2. Background

**2.1. Packing Efficiency Calculation.** Basic requirement when producing sensors is cost reduction by improving wafer productivity. This is defined as the fraction of the used wafer area to the total wafer area [31]. Szabo et al. [8] defined the density of a circle packing  $P(r, S)$ , where  $r$  is a radius of the inner circle and  $S$  is size of the square container. The PE of  $n$  packed circles is given by the formula:

$$d_n(r, S) = \frac{nr^2\pi}{S^2}. \quad (1)$$

This means that packing density can be expressed as the ratio between total area covered by the packed items and the area of the usable container [8]. We adopt the former formula to approximate SE.

**2.2. Related Work.** Many studies are done on maximizing wafer efficiency, mostly concentrating on square or rectangular sensors. A method for optimizing number of square cells that geometrically fit on a circular wafer and maximizing wafer yield is developed in [32]. Ferris-Prabhu presented in his work algebraic expressions that explicitly relate the number of produced cells to the wafer diameter and to the geometric parameters of the cells [33]. Some formulas are developed estimating how many cells of a given area will fit on a wafer and how much wafer area will be lost due to roundness of the wafer [34]. An iterative cutting procedure was developed for maximizing number of rectangular cells produced from six-inch and eight-inch wafers to maximize wafer utilization [35, 36].

Unlike in the field of sensor manufacturing where the region of interest is a circular silicon wafer or a container, the circular CMS detector represents region of interest that needs

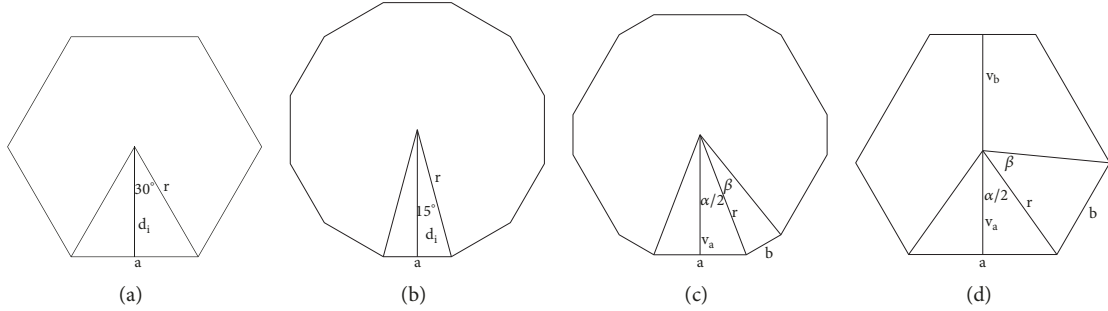


FIGURE 2: Defined sensor geometrical shapes: (a) regular hexagon, (b) regular dodecagon, (c) irregular dodecagon, and (d) irregular convex hexagon.

to be efficiently covered. Also, in the field of sensor networks, sensor positions are crucial in the form of a hexagonal grid to obtain better coverage efficiency and to cover the sensing area more efficiently [37]. The total number of sensors can be calculated using a known formula for centred hexagonal numbers defining a ring of hexagons [38, 39]. Kim et al. [40] apply a hexagon tessellation with an ideal cell size to deploy underwater WSN. Authors show that, for a circular region of interest, one can calculate the number of hexagon rings needed to fully cover the disk of a given radius.

There are many research problems on packing and various shapes of packed objects and containers are studied. Using rectangular or square container approximation is provided in the literature, concentrating mostly on circular packing problems. Litvinchev et al. [41] investigate the optimized packings of circles and “circular-like” objects in a rectangle to maximize the packed area and minimize waste. Authors simplify the packing problem by using a regular grid to model the inner positions of the packed items. This formulation is further adopted by [42, 43] and applied for cutting and packing of circles and ellipses. The goal is to pack as many items as possible to increase the efficiency and to decrease area of the container that needs to be produced.

Authors in [44] apply again a regular grid to a packing problem solution and derive a model for packing not only circles, but equal and unequal regular convex polygons such as hexagons in a rectangular region. Also, [45, 46] are devoted to efficient solutions for packing convex objects in the rectangular container. Different object shapes can be adjusted to the given packing schemes and minimize the cost by eliminating the unpacked areas.

**2.3. Contributions.** Despite using a rectangular container model as in the previous researches, it can be adjusted to handle some other geometrical shape such as polygon or circle. Provided solutions can support the simple change of different container approximations [47]. Authors in [48, 49] provide a heuristic approach to maximize the number of unit items such as rectangles, squares, or circles inside a circle of known radius. Also, the polygon-shaped or circular container is considered in [50, 51], with the aim to minimize the size of the polygon such that it contains a given set of fixed-size inner circles and ellipses and to increase the fraction of the packed container area.

In this paper, we adopt the idea of using a regular grid methodology to provide solutions of a packing problem. We present mathematical constructions to calculate the packing density of embedding regular and irregular hexagons and dodecagons in a circular container. Based on the literature search, none of the papers deal with these specific types of cutting polygonal sensor shapes. Hence, we address that specific type of packing problem when irregular hexagons and dodecagons are packed into circular container and we derive PE formulas.

We define four different sensor shapes produced from a circular silicon wafer, that are presented in Figure 2. Irregular dodecagon is gained from regular hexagon with small vertex cuts applied. Regular dodecagon is regular hexagon with maximal vertex cuts applied. We adopt the irregular hexagon with three symmetry axes in the triangular grid from [52]. We extend the possible irregular hexagon types with respect to their size defined by the sides  $a$  and  $b$ . We tessellate those hexagons to cover a given area of interest and compare the coverage efficiencies. We prove that silicone waste would be minimized when the ratio  $a/b$  is minimal. Increasing the ratio is proportional to silicone waste. We also compare the tessellated irregular hexagons with  $\{3, 12^2\}$  Archimedean semiregular tessellation. We show that SE is negligible; these irregular hexagonal sensors can be produced with SE almost as in the regular semiregular tessellation.

We provide a study in two directions; first, we analyze SE when  $N$  sensors are produced from a fixed-size circular container (for each of the four sensor types). When  $N = 1$ , it represents the case when producing a single sensor. Next, if all sensors are produced from the same wafer size, we compare SE when covering a circular surface that is flexible in size. Generally, we propose new formulations to develop a general model by using semiregular tessellation for the hexagon packing problem, giving the solution where the silicon waste is minimal.

### 3. Tessellation Method

**3.1. General Description.** A tiling or a tessellation is covering a flat surface using one or more tiles without any overlaps or gaps. Although the used tiles can have arbitrary shape, we focus on regular polygons (hexagons and dodecagons). Concerning the mathematical tiling context, edge is a boundary

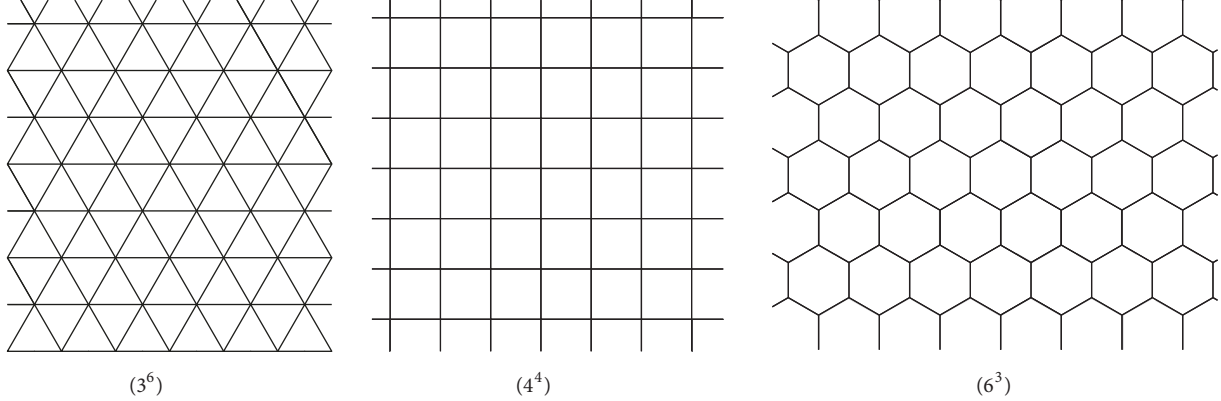


FIGURE 3: Three regular tessellations (adjusted from [53]).

which separates the two tiles, and vertex is an endpoint of an edge.

We say that a tiling of the plane is an *edge-to-edge tiling* if it uses polygons only and all adjacent tiles share full edges. We say that a tiling of the plane is *vertex-transitive* if it uses only polygons and every vertex (where three or more tiles are connected) is the same as any other vertex, in terms of the number, kind, and sequence of the shapes surrounding it.

Tiling is monohedral if all the tiles are of the same shape and size. Otherwise, it can be dihedral, trihedral, etc. Regular tiling is an edge-to-edge tiling by using congruent regular polygons. We could say it is a subtype of monohedral tiling. Uniform tiling is the tessellation of the plane by regular polygons with the restriction of being vertex-transitive. There are just three regular uniform tiling types given in Figure 3.

### 3.2. Regular Hexagon Tessellation

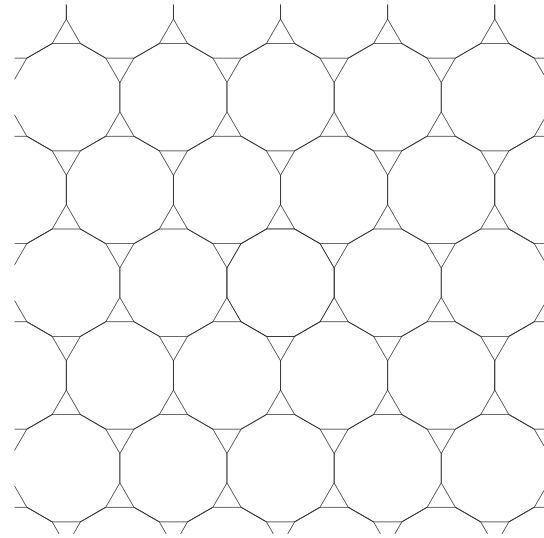
*Proof.* It is mathematically trivial to prove tessellation with regular hexagons. The sum of all angles in one vertex is 360°. The sum of the inner polygon angles is  $(n - 2) \cdot 180^\circ$ . As all inner angles are equal, it follows that  $\alpha_n = ((n - 2) \cdot 180^\circ)/n$ . There are  $k$  regular polygons in each vertex, and all the above can be represented with the following equation ( $n \geq 3$ ):

$$k \cdot \frac{(n - 2) \cdot 180^\circ}{n} = 360^\circ. \quad (2)$$

Relation (2) can be written as  $k = 2 + 4/(n - 2)$ , where there are possible solutions only for  $n \in \{3, 4, 6\}$ . In the case of regular hexagon where  $n = 6$ , it gives  $k = 3$  (number of hexagons in each vertex). The other possible solutions confirming tessellation are  $n = 4$  and  $n = 3$ .  $\square$

**3.3. Semiregular Tessellation.** Archimedean or semiregular tessellation uses more than one type of regular polygon with the restriction of being vertex-transitive.

*Proof.* We show the proof of the simplest possibility which allows usage of two different types of regular polygons in the tessellation. The following equation represents the fact that

FIGURE 4: Archimedean  $\{3, 12^2\}$  semiregular tessellation (adjusted from [54]).

single vertex is a meeting point for  $k_1$  regular polygons  $n_1$  and  $k_2$  regular polygons  $n_2$ :

$$k_1 \cdot \frac{(n_1 - 2) \cdot 180^\circ}{n_1} + k_2 \cdot \frac{(n_2 - 2) \cdot 180^\circ}{n_2} = 360^\circ, \quad (3)$$

where  $k_1, k_2, n_1, n_2 \in N$  and  $n_1, n_2 \geq 3$  (the smallest polygon  $n$  is a triangle). This can be also expressed as

$$k_1 \cdot \left( \frac{1}{2} - \frac{1}{n_1} \right) + k_2 \cdot \left( \frac{1}{2} - \frac{1}{n_2} \right) = 1. \quad (4)$$

One possible solution for (4) is when  $n_1 = 3$ ,  $n_2 = 12$  with  $k_1 = 1$ ,  $k_2 = 2$ , and each vertex is a meeting point for one equilateral triangle and two regular dodecagons. This is Archimedean  $\{3, 12^2\}$  semiregular tessellation, as shown in Figure 4. Last possible solution allows usage of three different types of regular polygons in tessellation (it is easy to prove that it is not possible to use more than three). With similar argumentation as in previous two cases, we conclude that there are eight possible semiregular tessellations [54].  $\square$

## 4. Methodology

**4.1. Research Problem.** Sensors are defined by four geometrical shapes, as shown in Figure 2. The packing problem of embedding sensors in a circular container can be explained with the following problem formulations:

- (i) *Problem 1.* Find the minimal circle radius  $R$  such that  $N$  equal sensors of known size can be fit inside.
- (ii) *Problem 2.* Find maximal size of a produced sensor, such that minimally  $N$  such sensors can be packed into a circular area of radius  $R$ .
- (iii) *Problem 3.* Find maximum number of sensors packed into a circular area with the known radius size.
- (iv) *Problem 4.* Derive PE (or SE) formulas.

**4.2. Research Context.** We use the following approach in solving the above problems. First, we start from a well-known regular hexagon tessellation and revisit the covering an area of interest without voids or gaps. We use formulas to find solutions for this general case when regular hexagons are packed in the circular container. Next, since this “perfect” regular tessellation is not satisfactory in our case, not providing spacings for mechanical apertures, we derive Archimedean  $\{3, 12^2\}$  semiregular tessellation from the regular hexagon tessellation. This is done by cutting equilateral triangles at the vertex which is common to three joined regular hexagons.

It is well known that PE is decreased when semiregular tessellation is applied with respect to the regular tessellation. The ratio is defined already for the problem of packing circles into a squared container [9]. Even though it is expected to obtain lower PE when semiregular tessellation is used, we are interested to calculate the ratio between the two to evaluate the difference of using regular and semiregular tessellation when packing sensors into a circle.

Because of the flexibility in choosing the size of the triangular spacings with lowering the side of a regular dodecagon, we move from the regular dodecagons to the irregular ones (with 6 symmetry axes). We study the efficiency when packing them into a circular container. Irregular dodecagons can provide us the desired PE, but with larger number of cuts when producing a single sensor (number of cuts is 12, compared to a regular hexagon that needs only 6 cuts in the production). Hence, we examine the possibility of the sensor to remain hexagonal in shape. We construct a sensor that is in a form of an irregular symmetric hexagon and we pack them in the circular area.

To minimize the number of needed cuts of the sensor and together with provided triangular spacings, we propose semiregular tessellation with irregular hexagons (with 3 symmetry axes) that is not edge-to edge. Our goal is to compare our proposed packing with other shapes semiregularly tessellating the plane, considering that triangles must be cut out by default, so that we can have a fair comparison. Finally, we compare PE for each sensor type.

**4.3. Research Questions.** The questions that need to be answered with this study are formed by two aspects:

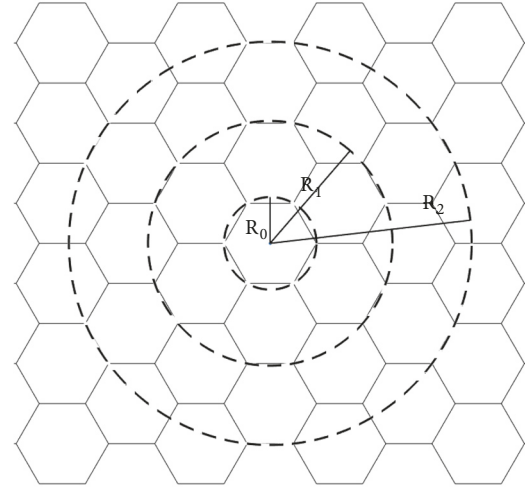


FIGURE 5: Regular hexagon rings.

- (i) Producing  $N$  sensors and calculating SE:

- (1)  $N = 1$ 
  - (a) Which one is the most efficient?
  - (b) Is producing an irregular hexagon cost-effective?
- (2)  $N > 1$ 
  - (a) What is the SE ratio between regular and semiregular tessellation?
  - (b) Is producing  $N$  irregular hexagons cost-effective?
- (ii) Packing sensors of known dimensions in the circular area of interest and calculating PE which represents coverage efficiency:
  - (1) Flexible-size container in which we always pack the same number of sensors
    - (a) Which sensor shape requires the container to be the smallest?
    - (b) Which sensor shape reduces the unused packed space in the container and increases PE when area of interest is covered?
    - (c) Which sensor shape enables that larger area of interest can be covered?

## 5. Packing Regular Polygons into Circle

**5.1. Regular Hexagon Tessellation in the Circular Area.** Let us consider the regular hexagon tessellation with the coordinate system set like it is shown in Figure 5. The circle of radius  $R$  centered in the coordinate system origin contains exactly one hexagon. We denote the central hexagon with  $k = 0$ . The nearest neighbors of the central hexagon create the first “hexagon ring,” denoted by  $k = 1$ .

Number of hexagons in a ring is equal to 6. If we denote the number of hexagons in  $k^{th}$  ring with  $N_k$ , we can see that

$N_0 = 1, N_1 = 6, N_2 = 12, N_3 = 18 \dots N_k = 6k$ . Therefore, the total number of hexagons starting from the origin until the  $k^{\text{th}}$  ring (included) will be

$$S_k = N_0 + N_1 + N_2 + \dots + N_k = 1 + 6 + 12 + \dots + 6k. \quad (5)$$

After summing the arithmetic sequence, we get the formula:

$$S_k = 3k^2 + 3k + 1. \quad (6)$$

With  $R_k$  we denote the radius of a circle containing ring  $k$  completely. Maximum distance from the hexagon vertex in  $k^{\text{th}}$  ring from the origin is  $R_k^2 = (a/2)^2 + (d_i + 2k \cdot d_i)^2$ , where the inner diameter  $d_i$  of hexagon is calculated with the relation  $d_i = a\sqrt{3}/2$ . Finally, we get the following:

$$R_k = a\sqrt{S_k} = a\sqrt{3k^2 + 3k + 1}. \quad (7)$$

*Solution (Problem 1).* Let us find the minimal value of radius  $R$  such that  $N$  equal nonoverlapping hexagons with known side value  $a$  can be packed inside. We will reformulate the problem: for exact number of regular hexagons  $N$  with side  $a$ , how many rings does it take to cover them completely? If we know the number of needed rings  $k$ , then according to (7) and (6), we also know  $R_k$ . Assumption

$$S_{k-1} \leq N < S_k \quad (8)$$

results in

$$k = \left\lfloor \frac{1}{2} + \frac{\sqrt{12N - 3}}{6} \right\rfloor. \quad (9)$$

Knowing the number of rings  $k$  in the tessellation, according to (7), it is easy to determine radius  $R = R_k$ .

*Solution (Problem 2).* Let us find the maximal size of a regular hexagon  $a$ , such that minimally  $N$  of them can be packed into a circular area  $C$  of radius  $R$ .

By using the same assumption (8) as in Problem 1, we come to the same conclusion about the number of needed rings (9). Using (7), it follows that  $a = R/\sqrt{3k^2 + 3k + 1}$ .

*Solution (Problem 3).* How many regular hexagons of side length  $a$  can be packed inside the circle with radius  $R$ ?

Again, we reformulate the problem: for a given circle of radius  $R$ , let us determine the maximum ring contained in that circle. In this case, assumption

$$R_{k-1} \leq R < R_k \quad (10)$$

with notation  $P = (R/a)^2$  gives

$$k = \left\lfloor \frac{1}{2} + \frac{\sqrt{12P - 3}}{6} \right\rfloor. \quad (11)$$

Using (6), the maximum number of packed sensors is  $N = S_{k-1} = 3k^2 - 3k - 2$ .

*Solution (Problem 4).* Let us derive the PE formula. The area of all hexagons from origin to the  $k^{\text{th}}$  ring  $A_k$  ( $S_k$  hexagons) is

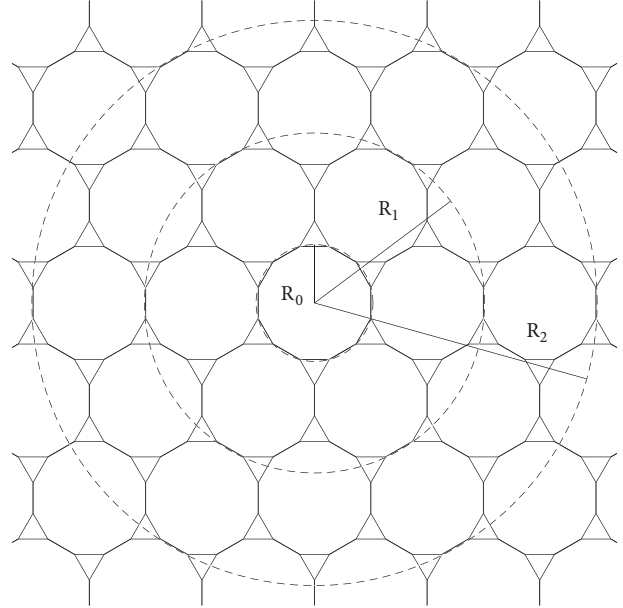


FIGURE 6: Regular dodecagon rings.

$A_k = S_k \cdot Ah$ , where  $Ah = (3\sqrt{3}/2)a^2$  is the area of a regular hexagon.

If we compare  $A_k$  with a circle containing  $k$  rings area  $C_k$ , we get the PE:

$$\frac{A_k}{C_k} = \frac{S_k \cdot Ah}{R_k^2 \pi} = \frac{3\sqrt{3}}{2\pi} \approx 0.83. \quad (12)$$

Thus, the ratio is constant and independent of  $k$  or  $a$  value.

**5.2. Archimedean Semiregular Tessellation.** Using the same logic with the notation like in the previous regular hexagon tessellation case, we derive problem solutions on Archimedean  $\{3, 12^2\}$  semiregular tessellation. The centre of the regular dodecagon's circumscribed circle is matched with the sensor centre (Figure 6). Dodecagons that are nearest neighbours to the central hexagon create a "dodecagon ring." It includes few equilateral triangles as well. The total number of dodecagons including the  $k^{\text{th}}$  ring is the same as in the hexagonal case (6).

If  $R_k$  is the radius of a circle containing ring  $k$  completely, then  $R_k^2 = (a/2)^2 + (d_i + 2k \cdot d_i)^2$ , where  $d_i$  is the inner diameter of the dodecagons  $d_i = (a/2)\tan 75^\circ$ . Finally, we get

$$R_k = \frac{a}{2} \sqrt{1 + \tan^2 75^\circ \cdot (2k + 1)^2}. \quad (13)$$

*Solution (Problem 1).* Assumption in this semiregular tessellation case will be the same as with the regular tessellation (8) and due to (6), the conclusion about the number of rings needed is the same as (9):  $k = \lfloor 1/2 + \sqrt{12N - 3}/6 \rfloor$ . For given  $k$ , using (15), we calculate  $R = R_k$ .

*Solution (Problem 2).* Let us find maximal size of a regular dodecagon, such that minimally  $N$  of them can be packed into a circular area  $C$  of radius  $R$ .

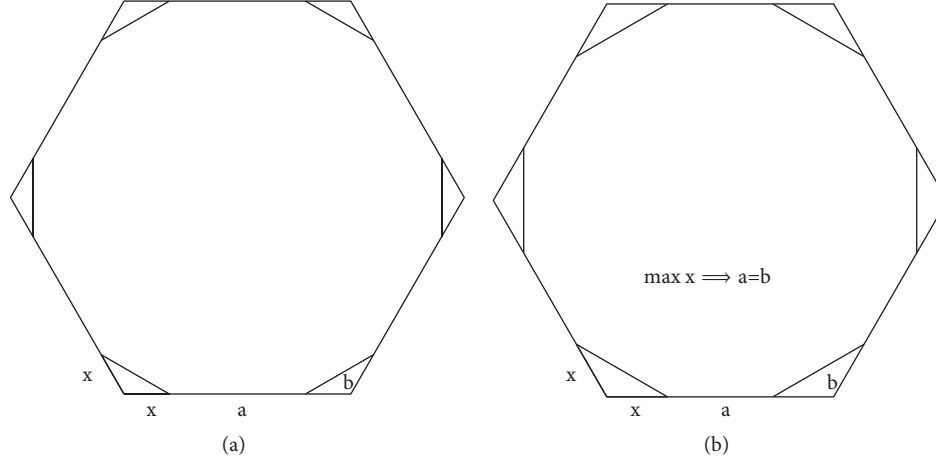


FIGURE 7: (a) Irregular dodecagon, cut from regular hexagon. (b) For maximum x-cut value, dodecagon is regular.

Applying the same logic as in regular tessellation, using (9) we calculate  $k$  such that  $R_k = R$ . By using (13), it follows that  $a = 2R_k/\sqrt{1 + \tan^2 75^\circ \cdot (2k+1)^2}$ .

*Solution (Problem 3).* How many regular dodecagons with side length  $a$  can be packed inside the circle with radius  $R$ ?

Again, we use the same logic as in the regular hexagon case. Assumption (10) with notation  $P = (2R/a)^2$  gives

$$k = \left\lfloor \frac{1}{2} \left( \cot 75^\circ \sqrt{P-1} + 1 \right) \right\rfloor. \quad (14)$$

Therefore, the maximum number of packed sensors for a given ring  $k$  is  $N = S_{k-1}$ .

*Solution (Problem 4).* Let us derive the PE formula. The area of a regular dodecagon is  $Ad = 3a^2 \tan 75^\circ$ . Consequently, the area of dodecagons from origin to the  $k^{th}$  ring is  $A_k = S_k \cdot Ad$ . If we compare  $A_k$  with area of circle containing  $k$  rings  $C_k$ , we get the PE:

$$\frac{A_k}{C_k} = \frac{S_k \cdot Ad}{R_k^2 \pi} = \frac{36S_k}{\pi [3\tan 15^\circ + 16S_k - 4]}. \quad (15)$$

Therefore, the ratio depends only on  $k$  value.

## 6. Packing Irregular Polygons into Circle

*6.1. Irregular Convex Dodecagon.* If we take regular hexagon and starting from each vertex, we move along the side for the same distance  $x$ , like it is shown in Figure 7, and finally we connect ending points, and we get irregular dodecagon. Regular dodecagon is just a special case where  $a = b$  which is true for the cut value  $x = a/(\sqrt{3} + 2)$ .

Let us now define the irregular dodecagon rings (Figure 8), whose number of contained sensors is the same as in all three previous cases. Maximum distance from irregular

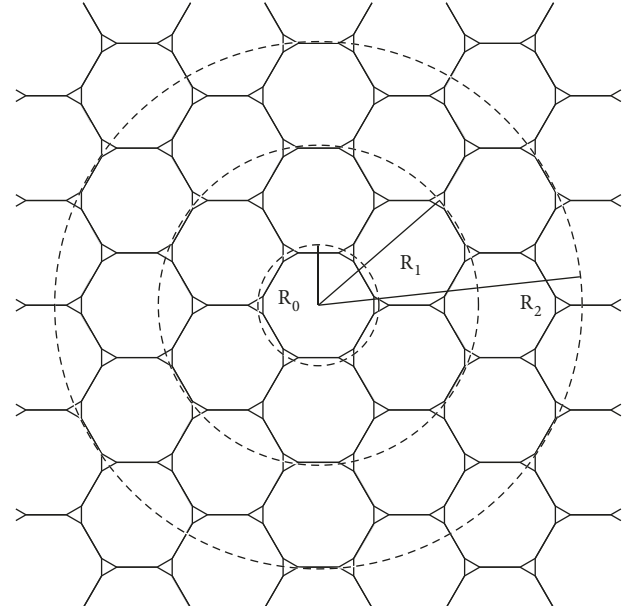
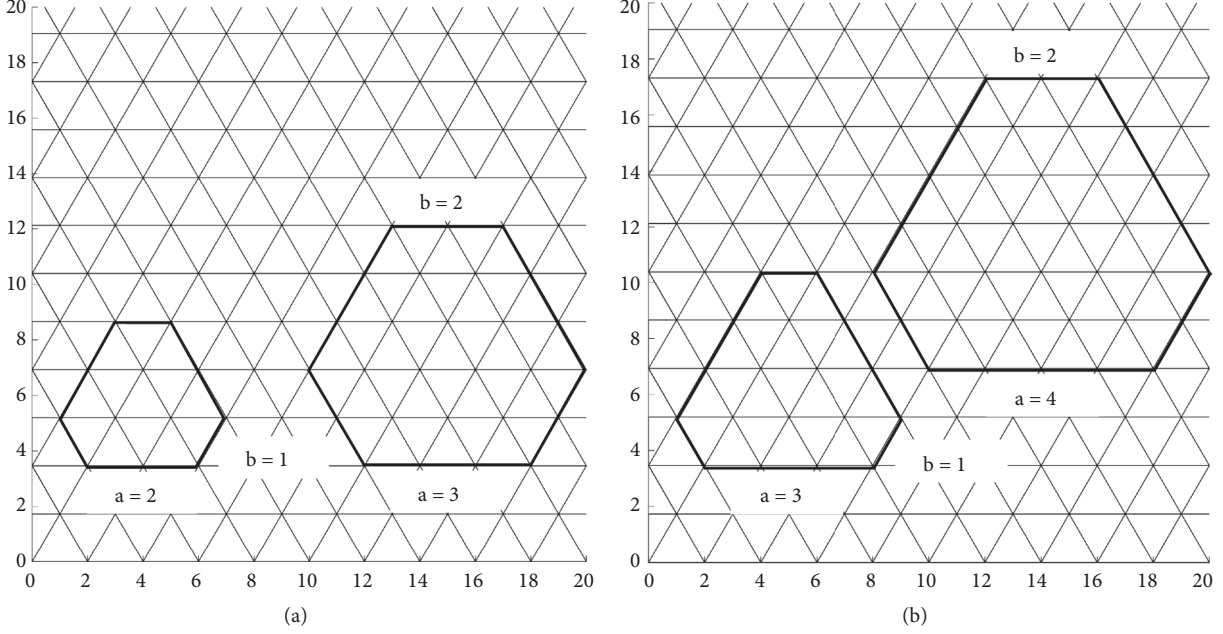


FIGURE 8: Irregular dodecagon rings.

dodecagon vertex in  $k^{th}$  ring from origin is  $R_k^2 = (a/2)^2 + (v_a + 2k \cdot v_a)^2$ . Using the fact that  $v_a = a/(2\tan(\alpha/2))$ , it follows that

$$R_k = \frac{a}{2} \sqrt{1 + \left( \frac{2k+1}{\tan(\alpha/2)} \right)^2}. \quad (16)$$

*Solution (Problem 1).* The number of dodecagons in each ring and total number of dodecagons  $S_k$  are the same as in Archimedean  $\{3, 12^2\}$  semiregular tessellation. Hence, by using the same assumption, the result about number of needed rings  $k$  is given by (9). For that  $k$  we calculate appropriate radius  $R = R_k$  using (16).

FIGURE 9: (a) Irregular hexagon  $H(1)$ , (b) irregular hexagon  $H(2)$ .

Triangular spacing is equilateral triangle with side  $b$  whose area is defined as  $P = b^2 \sqrt{3}/4$ .

*Solution (Problem 2).* Let us find the maximal size of a regular dodecagon, such that minimally  $N$  of them can be packed into a circular area  $C$  of radius  $R$ . Applying the same logic as in regular tessellation, using relation (9), we calculate  $k$  such that  $R_k = R$ . From (13), it follows that  $a = 2R_k/\sqrt{1 + ((2k+1)/\tan(\alpha/2))^2}$ .

*Solution (Problem 3).* Assumption (10) is used. With notation  $P = (2R/a)^2$  it gives

$$k = \left\lfloor \frac{1}{2} \left( \tan \frac{\alpha}{2} \sqrt{P-1} + 1 \right) \right\rfloor. \quad (17)$$

By using (6), the maximum number of packed sensors is  $N = S_{k-1}$ .

*Solution (Problem 4).* To calculate the PE formula, first we determine the area of an irregular dodecagon:  $Aid = 3r^2(\sin \alpha + \sin \beta)$ , where circumference circle radius  $r$  is calculated by  $r = a/(2 \sin(\alpha/2))$ . The area of all dodecagons contained from origin to  $k^{th}$  ring  $Ai_k$  is

$$A_k = S_k \cdot Aid = (3k^2 + 3k + 1) \cdot 3r^2 (\sin \alpha + \sin \beta). \quad (18)$$

Using (16) and because  $\alpha + \beta = 60^\circ$ , PE can be expressed as

$$\frac{A_k}{C_k} = \frac{3(3k^2 + 3k + 1) \cdot \cos(\alpha - 30^\circ)}{\pi (\sin^2(\alpha/2) + \cos^2(\alpha/2)(2k+1)^2)}. \quad (19)$$

**6.2. Irregular Convex Hexagon.** Let us consider an irregular convex hexagon  $H$  with three symmetry axes in the triangular coordinate system (Figures 9(a) and 9(b)).

The hexagonal shape below is adjusted from [40]. We define hexagon size by two parameters; sides  $a$  and  $b$ . The ratio  $a/b$  is fixed and it is defined by small triangle side ratio as shown in Figure 9. We extend the class of hexagons by increasing the ratio  $a/b$ , as shown in Figure 9. As we have already stated before, we construct irregular hexagon which decreases the number of cuts in the single sensor production and enables the flexibility of the triangular spacings. We define irregular hexagon types denoted with  $H(\Delta)$ , where  $\Delta = |a - b|$ .

We refer to irregular hexagon from Figure 9(a) as  $H(1)$  and from Figure 9(b) as  $H(2)$ , while hexagons in Figure 10 are referred to as  $H(4)$  and  $H(6)$ , respectively. From the relation  $\alpha + \beta = 120^\circ$  (refer to Figure 2(d)), it follows that

$$\tan \frac{\alpha}{2} = \frac{\sqrt{3}}{1 + 2(b/a)}. \quad (20)$$

Therefore, it is enough to know the ratio  $b/a$  (or  $a/b$ ) to determine the inner hexagon angles. For example, if  $a/b = 7/5$ , then it follows that  $\alpha \approx 71^\circ$  and  $\beta \approx 49^\circ$ .

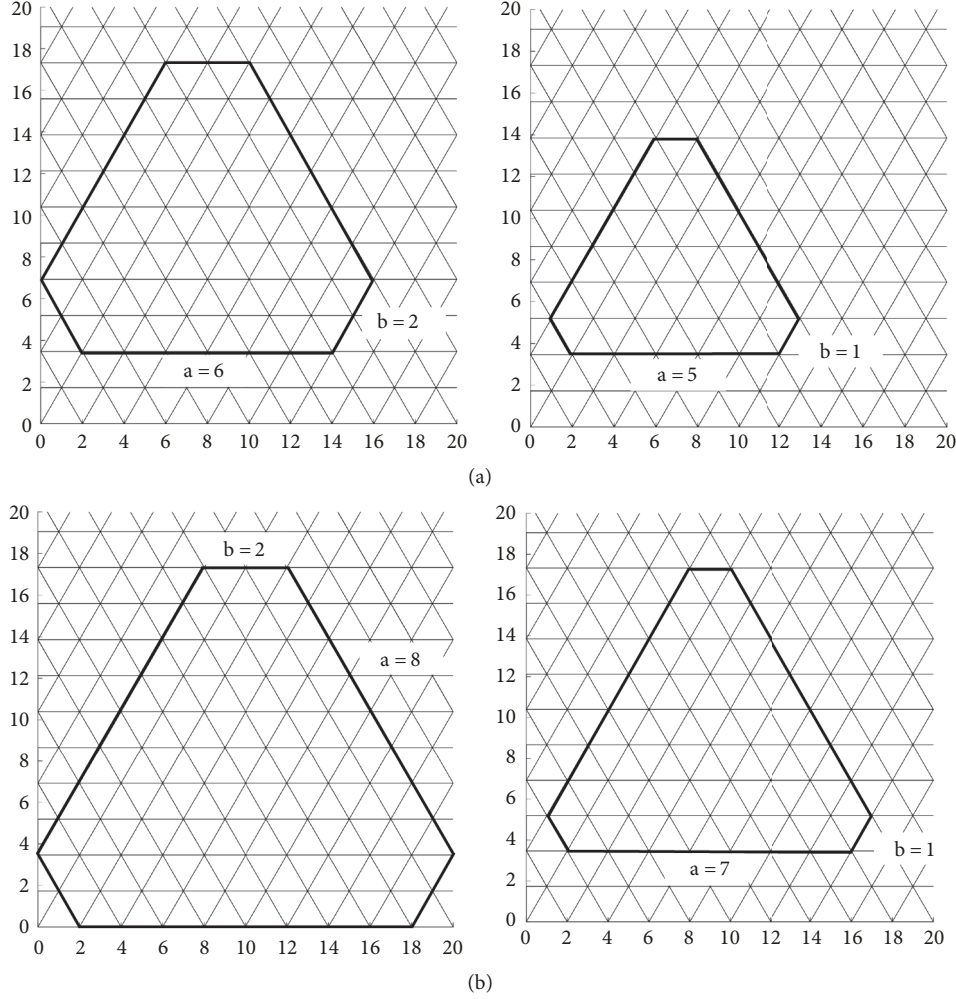
Triangular spacing is equilateral triangle with side  $x$  that is defined as  $x = \Delta/2$ . It follows that the triangle area is

$$P_x = \frac{\Delta^2 \sqrt{3}}{16}. \quad (21)$$

Therefore, based on the size of the triangular spacing, higher  $\Delta$  provides larger triangle area that gives larger waste in the sensor production, but it provides larger area for mechanical apertures when  $N$  sensors cover a circular area of interest.

For  $\alpha > \beta$ , the area of this irregular hexagon can be calculated by using the formula:

$$Aih = \frac{3\sqrt{3}}{2} r^2 \sin(150^\circ - \alpha), \quad (22)$$

FIGURE 10: Irregular hexagon. (a)  $H(4)$ ; (b)  $H(6)$ .

where circumscribed circle radius  $r$  is calculated as  $r = a/(2 \sin(\alpha/2))$ .

If we compare areas of the regular and irregular hexagon with the same circumscribed circle radius, we get

$$\frac{Ah}{Aih} = \frac{1}{\sin(150^\circ - \alpha)}. \quad (23)$$

Consequently, for the case where the ratio  $a/b = 7/5$ , it follows that  $Ah/Aih \approx 1/0.98$ . We can conclude that SE would be almost the same when one regular or irregular hexagon  $H(1)$  is produced from a circular wafer of a fixed radius.

We apply the same logic in describing irregular hexagon rings (Figure 11), as with regular hexagons used. The total number of hexagons starting from the origin until the  $k^{th}$  ring is again given by (6). With  $R_k$  we denote the circle radius that contains ring  $k$  completely, since maximum distance from hexagon vertex in  $k^{th}$  ring from origin is  $R_k^2 = (b/2)^2 + (\nu_b + k \cdot \nu_c)^2$ , where  $\nu_a + \nu_b = \nu_c$  (it is easy to show that  $R_k$  described using (shorter) side  $b$  has the higher value than the one with  $a$  side).

Parameters  $\nu_a, \nu_c$  are shown in Figure 2(d). Finally, it follows that

$$R_k = \frac{b}{2} \sqrt{1 + \left[ \operatorname{ctg} \frac{\beta}{2} \left( 1 + \frac{3}{2}k \right) + \frac{\sqrt{3}}{2}k \right]^2} \quad (24)$$

or using  $a/b$  ratio

$$R_k = \frac{b}{2} \sqrt{1 + \frac{1}{3} \left( (3k+1) + \frac{a}{b}(3k+2) \right)^2}. \quad (25)$$

*Solution (Problem 1).* For the irregular hexagon rings, the number of contained hexagons in each ring is the same as in the regular hexagon case. Thus, by using the same logic from (8), we come to the same number of needed rings (9). As for a given  $k$ , we can calculate the appropriate radius  $R = R_k$  by using (32).

*Solution (Problem 2).* Let us determine the maximal size of an irregular hexagon, such that minimally  $N$  of them can be packed into a circular area  $C$  of radius  $R$ . The same logic is

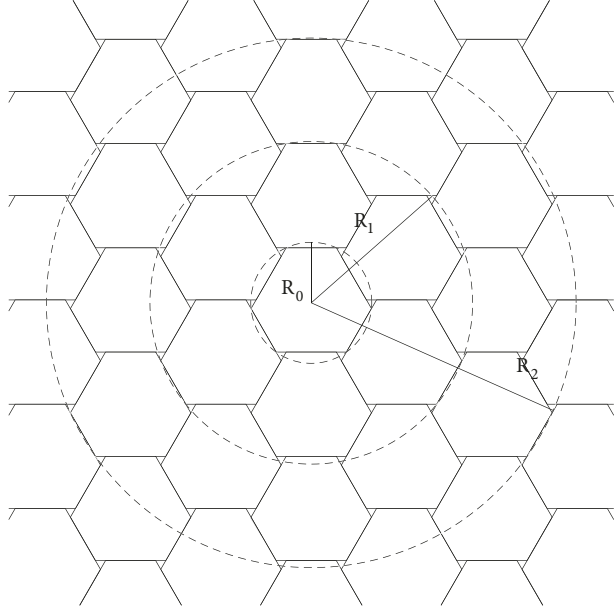


FIGURE 11: Irregular hexagon rings.

used as in solving previous Problem 2, which gives the needed number of rings  $k$  such that  $R_k = R$ .

In the previous discussion, we have narrowed the choice on irregular hexagons that have two different sides ( $a, b$ ) that alternate forming a symmetric geometrical shape. Irregular hexagons with different side values can have the same area. So, to determine the required type of irregular hexagon, we must know at least one of sides ( $a, b$ ) or  $a/b$  ratio. Therefore, by using (20) and (24) we get the needed values.

*Solution (Problem 3).* Again, assumption is formulated with the inequation (10). By using notation  $P = (2R/a)^2$  it follows that

$$k = \left\lfloor \frac{1}{3(1+a/b)} \left( \sqrt{3(P-1)} + 2 + \frac{a}{b} \right) \right\rfloor. \quad (26)$$

*Solution (Problem 4).* Let us derive the PE formula.

The area of an irregular hexagon  $H$  is  $A_{ih} = (3\sqrt{3}/2)r^2 \sin(150^\circ - \alpha)$ . The area of all hexagons from origin to  $k^{th}$  ring  $A_k$  ( $S_k$  hexagons in total) can be expressed as

$$\begin{aligned} A_k &= S_k \cdot A_{ih} \\ &= (3k^2 + 3k + 1) \cdot \frac{3\sqrt{3}}{2} r^2 \sin(150^\circ - \alpha). \end{aligned} \quad (27)$$

If we compare the area of one circle containing  $k$  rings  $R_k$ , with area  $A_k$  we get the PE:

$$\begin{aligned} \frac{A_k}{C_k} &= \frac{3\sqrt{3}S_k \sin(30^\circ + \beta)}{2\pi \left[ 1 + [\operatorname{ctg}(\beta/2)(1 + (3/2)k) + (\sqrt{3}/2)k]^2 \right] \sin^2(\beta/2)}. \end{aligned} \quad (28)$$

Thus, the ratio depends on  $k$  and  $\beta$  value.

## 7. Results and Discussion

PE is calculated with using every sensor geometrical shape, approximating SE in the sensor production cost and PE which represents coverage efficiency when packing sensors of known dimensions in the circular area of interest. In the former context, we separate the following cases:

- (a) A single sensor ( $N = 1$ ) is produced by a fixed-size circular silicon wafer given by radius  $R$ .
- (b)  $N$  sensors are produced ( $N > 1$ ) by a fixed-size circular silicon wafer given by radius  $R$ .
- (c) Sensors are produced from the fixed wafer size and they are packed into a circular container whose size is flexible. It is defined with the condition that always a fixed number of sensors  $N$  is contained inside ( $k$  sensor rings).

**7.1. Single Sensor Packing in Circle ( $N = 1$ ).** When a single sensor is produced, one must consider the useful wafer area available in the manufacturing process, as shown in Figure 12. SE is the largest for dodecagon sensor shape ( $\approx 96\%$ ) since it is the closest to the circle, while for regular hexagon SE  $\approx 83\%$ .

When the proposed irregular hexagon  $H(\Delta)$  is used, efficiency is presented in Figure 13 which is in concordance with the area ratios presented in Figure 14. Naturally, based on relation (20), when  $b/a$  approaches the value 1,  $H(\Delta)$  approaches the SE of a regular hexagon as  $\alpha$  approaches  $60^\circ$  angle (Figure 15). Naturally,  $H(1)$  is the closest to the regular hexagon, so it obtains the highest SE (where the minimal value is  $\approx 80\%$ ). Hence, silicon waste is negligible when using this type of irregular hexagonal shape with respect to a regular hexagon. However, it is shown that using other irregular hexagons is also efficient. We can see in Figure 13 that  $SE > 55\%$  for  $\Delta \leq 5$ , which means that more than half of the wafer is utilized.

For a single sensor in the selected class of irregular hexagons (or for a specific  $\Delta$ ), it is possible to calculate needed criteria to satisfy the required SE. It follows that

$$\frac{A_0}{C_0} = \frac{3\sqrt{3} \sin(150^\circ - \alpha)}{2\pi} = \frac{3\sqrt{3} \sin(5\pi/6 - \alpha)}{2\pi}. \quad (29)$$

We can see from the above formula (29) that SE depends on the angle  $\alpha$  and this formula is true for every  $\Delta$ . Hence, we can see for the specific  $\Delta$  which ratios  $a/b$  are satisfactory. For example, if required SE is 75%, the above formula gives the angle  $\alpha < 1.4821$  or  $\alpha < 84.92^\circ$ . This means that, in  $H(3)$ , the required SE is achieved for  $b \geq 3$ .

Since regular dodecagon is the closest to the circular shape (Figure 12), it is reasonable to conclude that, when comparing a single sensor production in the regular and irregular dodecagons used (with increased ratios  $a/b > 1$ ), SE will be decreasing.

### 7.2. Comparison of Hexagon Packings ( $N > 1$ )

**7.2.1. Regular and Semiregular Tessellation.** When  $N$  sensors are produced from a fixed-size wafer, we use mathematical tessellation mechanism with centered-centric approach,

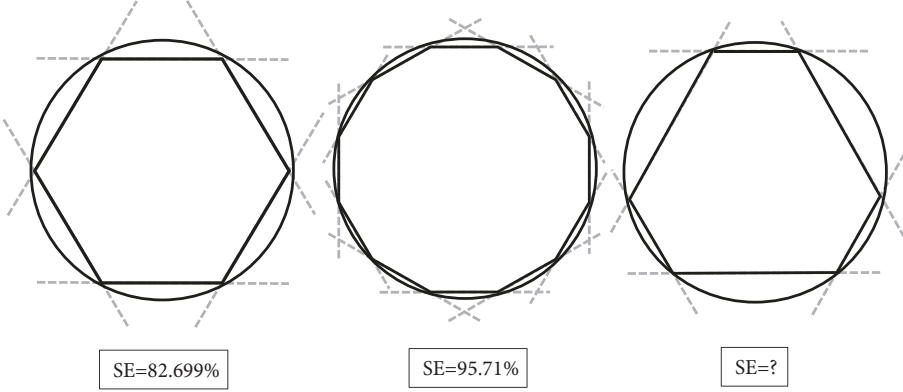


FIGURE 12: Straight lines applied in single sensor production.

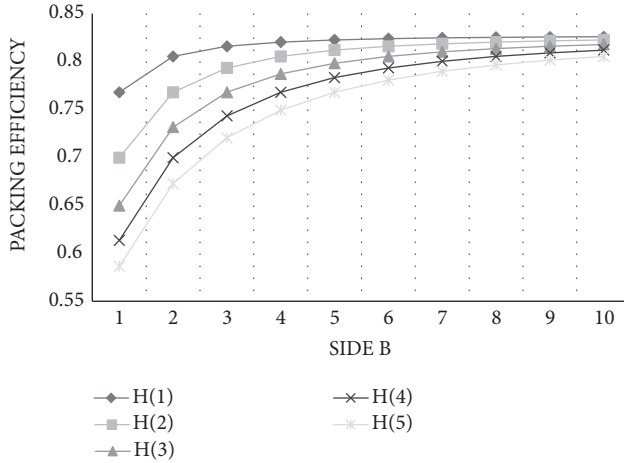
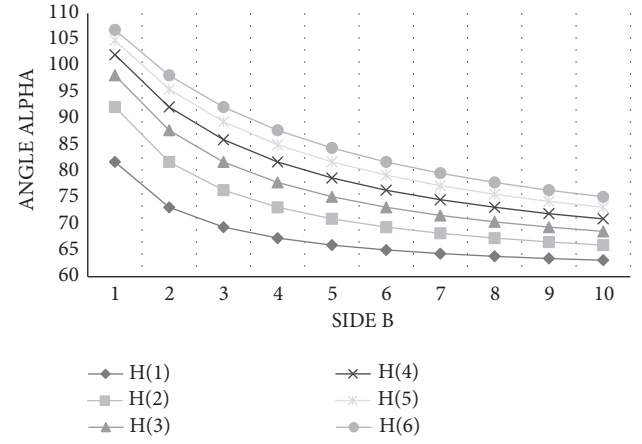
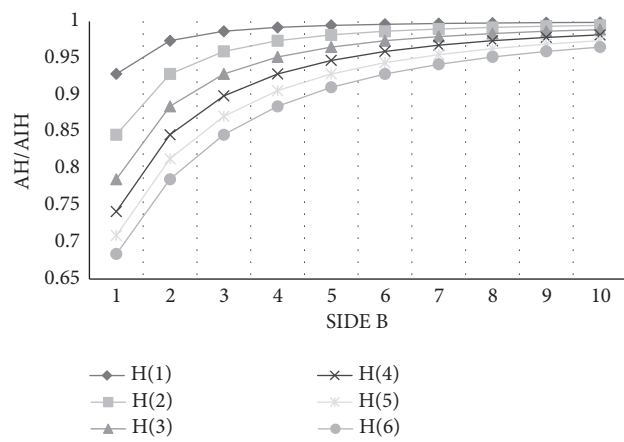
FIGURE 13: SE for irregular hexagon  $H(\Delta)$ ,  $\Delta = 1, 2, 3, 4, 5$ .FIGURE 15: Irregular hexagon  $H(\Delta)$  angle  $\alpha$ .

FIGURE 14: Comparison of regular and irregular hexagon area.

meaning that central sensor centre corresponds to the wafer centre. We form a requirement that

$$N \leq S_k. \quad (30)$$

This means that maximal number of sensors that can be produced is always limited by the number of rings  $k$ , as we want sensors to be tessellated inside the circular area. Also, it means that in the case where  $N \neq S_k$ , even if we need only  $N$  sensors, more sensors need to be produced. Thus, we calculate the sensor dimensions, such that  $k$  rings of them can be fit inside a fixed-radius and calculate the used PE (SE).

As we can see in Table 1, PE is constant for regular tessellation (83%), while Archimedean semiregular tessellation with regular dodecagon has  $SE \approx 77\%$ . Since regular dodecagon is larger for  $k = 0$  than a regular hexagon, its area becomes smaller compared to a regular hexagon when larger number of rings is packed in the same circular area. This causes lower PE with Archimedean semiregular tessellation used. This is expected, because silicon waste in the semiregularly tessellated case is obtained by cutting triangles at the sensor vertices.

Let us compare several semiregular tessellations with irregular dodecagons used, where smaller triangles are cut than in the case of Archimedean tessellation. We can see in Figure 16 that the larger the ratio is between sides of an irregular dodecagon, the more we approach to the efficiency of the regular tessellation. This is a natural conclusion

TABLE 1: Regular Hexagon and Regular Dodecagon for 8" wafer (R=100 mm).

k	$S_k$	Regular hexagon			Regular dodecagon		
		a [mm]	$A_h$	SE	a [mm]	$A_d$	SE
0	1	100	25980.8	0.827	51.8	30004.01	0.955
1	7	37.8	3711.5	0.827	17.8	3544.9	0.789
2	19	22.94	1367.4	0.827	10.7	1282.7	0.776
3	37	16.4	702.2	0.827	7.7	655.3	0.772
4	61	12.8	425.9	0.827	5.95	396.7	0.770
5	91	10.5	285.5	0.827	4.9	265.6	0.769
6	127	8.9	204.6	0.827	4.12	190.2	0.769
7	169	7.7	153.7	0.827	3.6	142.9	0.769
8	217	6.8	119.7	0.827	3.15	111.2	0.768
9	271	6.07	95.9	0.827	2.8	89.1	0.768
10	331	5.5	78.5	0.827	2.6	72.9	0.768

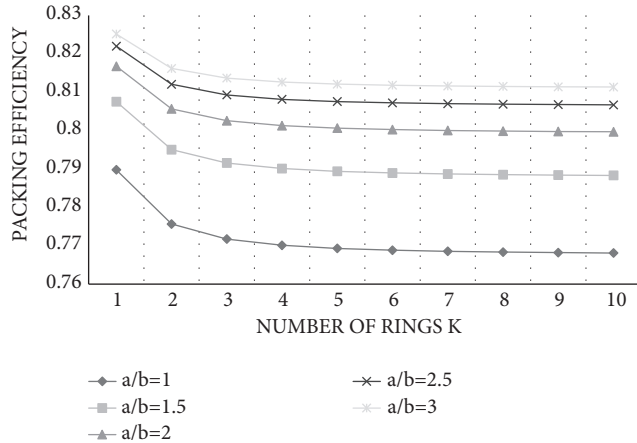


FIGURE 16: SE for semiregular tessellations with dodecagons (8" wafer, R=100 mm).

from the fact that when the side  $a/b$  ratio in the irregular dodecagon is larger, smaller triangles are cut at the vertices, causing the smaller amount of silicon waste. This is because the cut triangle side is  $b$ , so smaller size means smaller area and larger ratio  $a/b$ .

Maximal waste is obtained for the Archimedean semiregular tessellation, since maximal triangles are cut out from the wafer, causing the largest silicon waste.

**7.2.2. Irregular Hexagon.** When producing  $N$  sensors that are irregular hexagons, we can see that, with the increasing number of rings  $k$  packed in the circular wafer, SE is increasing, while this was not the case with the irregular dodecagon. The approximated value is based on the following limit functions, for irregular hexagon and irregular dodecagon, respectively:

$$\lim_{k \rightarrow \infty} \frac{A_k}{S_k} = \frac{3\sqrt{3}}{2\pi} \frac{\sin(30^\circ + \beta)}{\cos^2(30^\circ - \beta/2)} \quad (31)$$

$$\lim_{k \rightarrow \infty} \frac{A_k}{S_k} = \frac{9}{4\pi} \frac{\cos(\alpha - 30^\circ)}{\cos^2(\alpha/2)} = \frac{9}{4\pi} \frac{\cos(30^\circ - \beta)}{\cos^2(30^\circ - \beta/2)}. \quad (32)$$

It is already shown that SE is decreasing with the increased  $\Delta$  (Figure 13), and we confirm this again in Figure 17 graphs. We see that, based on relation (20), as  $\Delta$  is larger, the ratio  $b/a$  approaches zero, getting  $H(\Delta)$  further away from the SE of a regular hexagon. Naturally,  $H(1)$  is the most efficient. We can obtain larger SE when increasing the ratio  $b/a$  for the individual irregular hexagon architecture with  $\Delta > 1$ .

SE of the  $N$  produced irregular hexagons is larger when the number of sensor rings  $k \geq 4$ , than in the case of Archimedean  $\{3, 12^2\}$  semiregular tessellation where  $SE \approx 77\%$ . This is the case

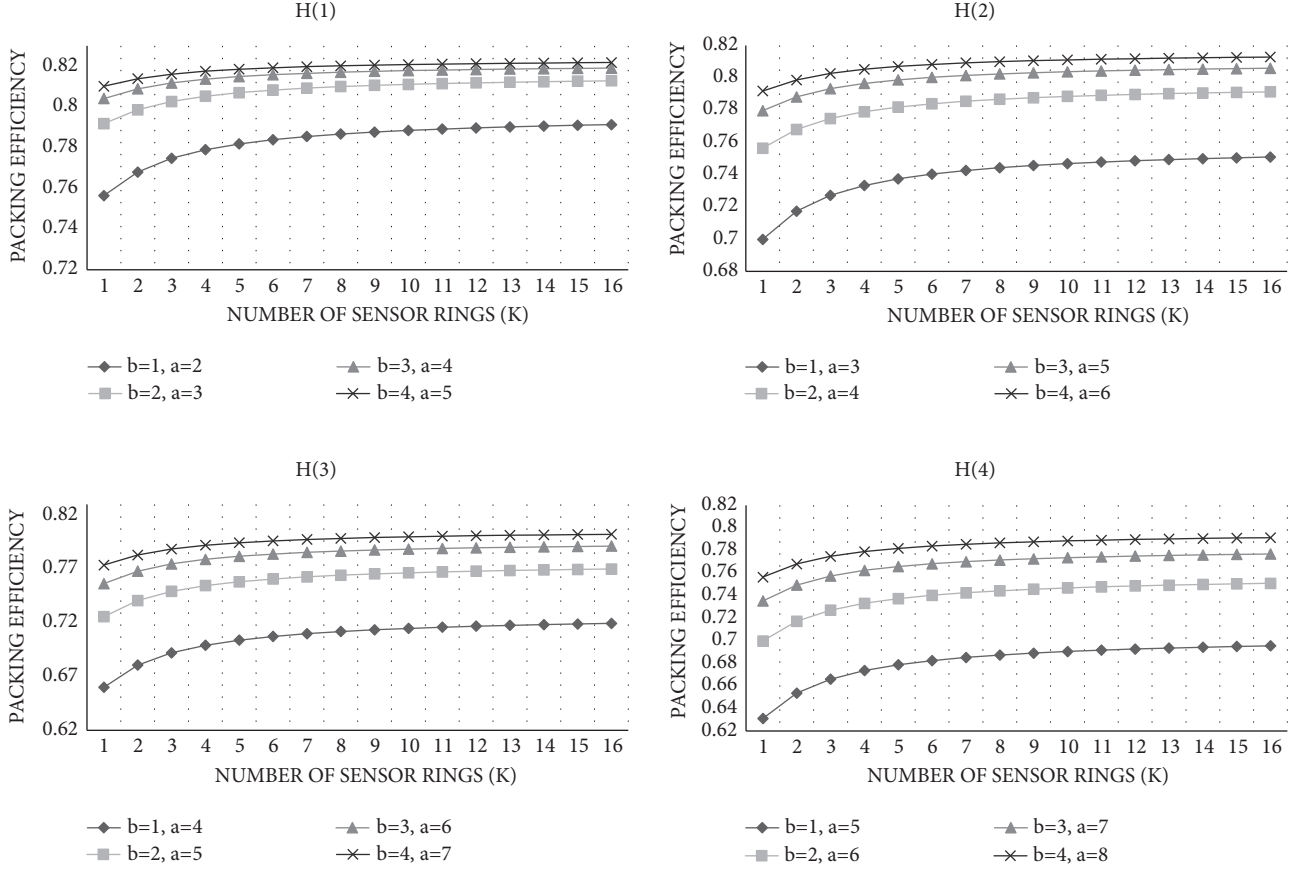
- (i) for every  $b/a$  ratio in  $H(1)$
- (ii)  $b/a \geq 0.5$  in  $H(2), H(3), H(4)$ .

For lower number of sensor rings  $k < 4$ , irregular hexagon would be almost as efficient as Archimedean semiregular tessellation for any  $\Delta$ . However, if one needs to obtain larger SE, it can be accomplished with  $b/a$  selected accordingly, such that it is closer to a regular hexagon.

We can conclude that one can produce  $N$  irregular hexagons with packing almost as efficient or even more efficient than in the case when using Archimedean semiregular tessellation. We can further increase the efficiency by using some other more efficient semiregular tessellation with irregular dodecagons, when smaller triangles are cut out at the vertices, but the number of cuts when producing a single dodecagonal sensor is double.

According to (21), we can see that the size of the triangular spacing depends on  $\Delta$ , where these two variables are proportional. When  $H(\Delta)$  is increased, the triangular spacing is increasing as well, causing larger amount of waste when  $N$  irregular sensors are produced from the circular wafer. This decreases the SE but requires minimal number of cuts when a single sensor is produced. Also, it increases triangular spacings for mechanical apertures where PE in covering a circular area remains satisfactory.

**7.3. Packing Fixed-Size Sensors into a Circular Container.** This section will obtain the same PE results as the efficiency in the previous one expressed in a form of SE. Namely, when

FIGURE 17: SE for irregular hexagon  $H(\Delta)$ ,  $\Delta=1, 2, 3, 4$ .

sensor size is fixed, and the area of the container is adjusted accordingly, this is the same as when we have a fixed region of interest and we adjust the sensor size. The reason is that we always use the centred tessellation approach defined by the number of sensor rings  $k$ .

When sensors are produced from the fixed-size wafers and we pack them in the circular container, we can discuss the size of the container that is required. Namely, the size of the container is flexible because we want to pack sensors of fixed dimensions with the centred tessellation mechanism and the restriction that all packed sensors are whole, there are no partial sensors. The size of a container is always defined such that a fixed and tessellated number of sensors with the valid restriction (30) can be fit inside.

When the size of the container is defined by the number of sensor rings that are packed inside, PE is the smallest for regular dodecagon or Archimedean semiregular tessellation. This means that leaving largest triangles unused in the sensor vertices causes the smallest coverage of the circular surface. On the other hand, we get the largest spacing area for mechanical apertures, but individual sensors are produced with maximal number of cuts. Using larger irregular dodecagons (like in the previous section) can reduce the unused packed space because triangular spacings are smaller, which increases PE towards the most efficient regular hexagonal tessellation used

(83%). However, triangular spacings are smaller and again we need to apply maximal number of cuts in a single sensor production.

Concluded from Figure 17, irregular hexagonal sensor shape will reduce the unused packed space in the container and increases PE when area of interest is covered. PE will be larger than Archimedean semiregular tessellation, with smaller triangular spacings, but these are provided naturally by the packing process. There are no cuts needed at the regular hexagon vertices since a single irregular hexagon sensor can be produced with minimal number of six cuts in total.

We can compare the size of the container that we need depending on how many sensor rings do we pack inside. Sensor is produced from a fixed-size wafer and example for 6" sensors is given in Figure 18(b). Since wafer radius is the same for all sensor shapes, regular dodecagon will require the largest container (because we assume that all sensors must be whole with no partial sensors allowed). The reason for this is that regular dodecagon is the largest in area and the closest to a circular shape. Hence, regular dodecagon shape enables that the largest area of interest can be covered.

Irregular dodecagons packed in the container cause the fact that its size can be smaller, and closer to the size of the container when regular hexagons are used. In this case,

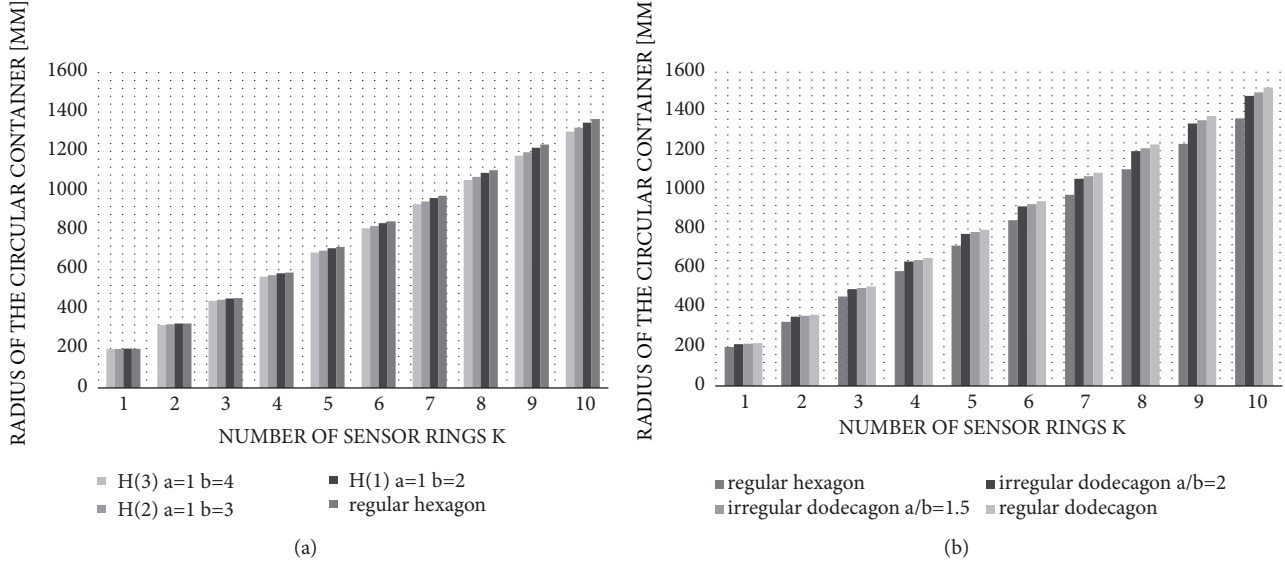


FIGURE 18: Size of the flexible container used for packing (6" wafer,  $R=75$  mm) compared to a regular hexagon. (a) Irregular hexagons, (b) irregular dodecagons.

the smallest container can be used for packing since regular hexagons have the largest PE. On the other hand, since the area of an irregular hexagon is smaller than the area of a regular hexagon, smaller container is needed for the same number of sensors that are packed inside (Figure 18(a)). The drawback can be that the same number of smaller sensors can cover smaller area of interest. This means that we place the same number of smaller sensors in the container knowing that its size will be smaller, covering the smaller area with the chosen sensor types.

## 8. Conclusions

Regular tessellation enables area to be covered with no voids or gaps, ensuring the constant  $PE \approx 83\%$ . Also, the same SE is obtained when a single sensor is produced in a form of a regular hexagon. In this “perfect” tessellation, one important drawback is that there are no spacings for mechanical apertures and mounting, when  $N$  such produced sensors are packed inside the circular area. This is needed in a specific application such as the design of the new CMS detector [1]. The spacings can be obtained with truncated tips at the vertices of the hexagonal sensors. When using these sensors with cut out maximal triangles at the vertices, we semiregularly tessellate the area of interest causing Archimedean  $\{3, 12^2\}$  semiregular tessellation. This way, sensor becomes a regular dodecagon. Also, using irregular dodecagonal sensor shape can provide us with some additional flexibility in adjusting the size of the triangular spacings, where lowering the spacing area causes the enhanced PE of the area.

Producing such dodecagonal sensors ( $N = 1$ ) is cost-effective in terms of silicone material, since SE of a regular dodecagon is larger than a regular hexagon, i.e.,  $SE = 95\%$ . On the other hand, producing single irregular dodecagons

increases the waste as expected. However, we can produce larger number of smaller sensors from a fixed-size circular wafer in the centred tessellated manner. The SE of a regular hexagon remains constant, and we derived the ratio between  $SE_{reg,hex} \approx 83\%$  and  $SE_{reg,dode} \approx 77\%$ , when  $N$  sensors are produced. Naturally, SE is increased with using dodecagonal sensor shapes, as waste of the silicon material is smaller.

The number of cuts needed in producing a single sensor is increased in double when dodecagon sensor shape is used compared with hexagon. Therefore, in this paper, we answered the question if we can use some other more efficient sensor shape that keeps the SE almost as if a regular hexagon was used, while the number of straight cuts when sensors are produced is minimal. With the proposed irregular hexagons, providing triangular space is enabled by default with semiregular tessellation and applying the vertex cuts on the sensors is avoided. The number of cuts needed in the sensor production is reduced because sensor remains hexagonal, even though irregular in shape. Choosing a specific group of irregular hexagons  $H(\Delta)$  enables us to decide on the size of the required triangular spacing with the PE that remains satisfactory. SE of producing a single irregular hexagonal sensor is satisfactory for  $\Delta = 1, 2, 3$  with  $SE > 65\%$ , with the largest efficiency obtained for the smallest  $\Delta = 1$ . Also, producing  $N$  such sensors is cost-effective, with the SE larger than Archimedean semiregular tessellation. The efficiency is growing with larger number of sensor rings produced, which is not the case in dodecagonal sensors used. When more sensors are produced, SE is getting closer to the desired 83% of a regular hexagon, which means that we can produce these sensors with almost the same SE.

Considering a specific application when produced sensors need to cover the circular area of interest with the satisfactory PE while providing triangular spacings for mechanical apertures, we conclude that regular dodecagons provide

the largest area to be covered. From the other point of view, it requires the largest container. Irregular hexagons on the other hand require the smallest container as they are smaller in area. Triangular spacings are provided by default in the packing procedure. We can adjust PE with different ratios  $b/a$  selected, such that it is closer to using a regular hexagon. Basically, we are adjusting the size of the gaps for mechanical apertures and mounting, while PE remains satisfactory.

As future work, we will observe a more realistic case where a problem of packing fixed-size sensors in a fixed-size container is studied. When sensors are produced from a fixed-size wafer and we aim to pack them into a fixed container, we first need to calculate how many of them can be fit inside. Then, based on a requirement (30) since we assort sensors in the tessellated manner, we can compare the obtained PE. It would be also interesting to repeat the study with the packing problem where noncentred tessellation is applied. Improved SE and PE can be expected since central sensor centre is moved with respect to the centre of the container.

## Data Availability

The data used to support the findings of this study is generated based on the formulas included within the article.

## Conflicts of Interest

The authors declare that there are no conflicts of interest regarding the publication of this paper.

## References

- [1] CMS Collaboration, Conceptual design report for the us hlc upgrade of the compact muon solenoid, [http://home.fnal.gov/~acanepa/uscms-hlup-cdr\\_26March.pdf](http://home.fnal.gov/~acanepa/uscms-hlup-cdr_26March.pdf), 2017.
- [2] I. Litvinchev and E. L. Ozuna Espinosa, “Integer programming formulations for approximate packing circles in a rectangular container,” *Mathematical Problems in Engineering*, vol. 2014, Article ID 317697, 6 pages, 2014.
- [3] I. Litvinchev, L. Infante, and E. L. Ozuna EspinosaL, “Approximate circle packing in a rectangular container: integer programming formulations and valid inequalities,” in *Computational Logistics (ICCL 2014)*, R. G. González-Ramírez, F. Schulte, S. Voß, and J. A. Cerón Díaz, Eds., vol. 8760 of *Lecture Notes in Computer Science*, Springer, 2014.
- [4] R. Torres-Escobar, J. A. Marmolejo-Saucedo, and I. Litvinchev, “Linear models for non-congruent circle packing in a rectangular container,” *International Journal of Applied Engineering Research*, vol. 13, no. 3, pp. 1784–1790, 2018.
- [5] T. Martinez, L. Vitorino, F. Fages, and A. Aggoun, “On solving mixed shapes packing problems by continuous optimization with the CMA evolution strategy,” in *Proceedings of the 1st BRICS Countries Congress on Computational Intelligence, BRICS-CCI 2013*, pp. 515–521, IEEE, Brazil, September 2013.
- [6] C. Uhler and S. J. Wright, “Packing ellipsoids with overlap,” *SIAM Review*, vol. 55, no. 4, pp. 671–706, 2013.
- [7] R. A. Merriam and V. D. Phillips, “Packing: useful tool for planted forest management. Weinrub A.(cur.),” in *Proceedings of symposium on systems and models in forestry, Punta de Tralca, Punta de Tralca, Chile*, 2002.
- [8] P. G. Szabo, M. C. Markot, T. Csendes, E. Specht, L. G. Casado, and I. Garcia, “New approaches to circle packing in a square: with program codes,” in *Optimization and Its Applications*, vol. 6, Springer, New York, NY, USA, 2007.
- [9] R. Williams, “Circle packings, plane tessellations, and networks,” in *The Geometrical Foundation of Natural Structure. A Source Book of Design*, pp. 34–47, Dover, New York, NY, USA, 1979.
- [10] P. G. Szabó, M. C. Markót, and T. Csendes, “Global optimization in geometry—circle packing into the square,” in *Essays and Surveys in Global Optimization*, pp. 233–265, Springer, Boston, Mass, USA, 2005.
- [11] H. In-Ting, Improvements on circle packing algorithms in two-dimensional cross-sectional areas, 2015.
- [12] L. Fukshansky, “Revisiting the hexagonal lattice: on optimal lattice circle packing,” *Elemente der Mathematik*, vol. 66, no. 1, pp. 1–9, 2011.
- [13] H. C. Chang and L. C. Wang, A simple proof of Thue’s theorem on circle packing, pp. 1–4, <https://arxiv.org/abs/1009.4322>, 2010.
- [14] S. Seok, *Advanced Packaging and Manufacturing Technology Based on Adhesion Engineering: Wafer-Level Transfer Packaging and Fabrication Techniques Using Interface Energy Control Method*, Springer, 2018.
- [15] E. Manea, E. Budianu, M. Purica et al., “Optimization of front surface texturing processes for high-efficiency silicon solar cells,” *Solar Energy Materials & Solar Cells*, vol. 87, no. 1–4, pp. 423–431, 2005.
- [16] S. N. Farrens, “Packaging methods and techniques for MOEMS and MEMS,” in *Proceedings of the MOEMS-MEMS Micro & Nanofabrication*, vol. 5716, San Jose, Calif, USA, 2005.
- [17] P. S. Hepsibha and G. S. Rao, “Comparative analysis of area coverage in wsns using various grid-based node deployment schemes,” *International Journal of Future Computer and Communication*, vol. 2, no. 6, pp. 633–637, 2013.
- [18] E. Donkoh and A. Opoku, “Optimal geometric disks covering using tessellable regular polygons,” *Journal of Mathematics Research*, vol. 8, no. 25, 2016.
- [19] K. J. M. Wang and M. W. Sze, *Semiconductor Die for Increasing Yield and Usable Wafer Area*, United States Patent Application Publication, 2008.
- [20] S. Bothra, Hexagonal Semiconductor Die, Semiconductor Substrates, and Methods of Forming a Semiconductor Die, United States patent 6,030,885, Feb. 29, 2000.
- [21] T. H. Daubenspeck, W. T. Motsiff, C. D. Muzzy, and W. Sauter, Patent No. 6,924,210. Washington, DC: U.S. Patent and Trademark Office, 2005.
- [22] J. E. Beasley, “An exact two-dimensional nonguillotine cutting tree search procedure,” *Operations Research*, vol. 33, no. 1, pp. 49–64, 1985.
- [23] G. M. Grivna and M. J. Seddon, U.S. Patent No. 9,165,833. Washington, DC: U.S. Patent and Trademark Office, 2015.
- [24] H. Okamoto, H. Tamemoto, and J. Narita, Method for manufacturing semiconductor element, U.S. Patent Application No 15/196,787, 2017.
- [25] T. J. Davis and T. Sinha, U.S. Patent No. 9,911,716. Washington, DC: U.S. Patent and Trademark Office, 2018.
- [26] W. Wen and S. Khatibi, “Virtual deformable image sensors: towards to a general framework for image sensors with flexible grids and forms,” *Sensors*, vol. 18, no. 6, article 1856, 2018.

- [27] R. Manthey, T. Schlosser, and D. Kowerko, “Generation of images with hexagonal tessellation using common digital cameras,” in *Proceedings of the IBS International Summerschool on Computer Science, Computer Engineering and Education Technology*, 2017.
- [28] A. Steen, “The CMS HGCAL detector for HL-LHC upgrade,” in *Proceedings of the The European Physical Society Conference on High Energy Physics*, vol. 521, Venice, Italy, July 2017.
- [29] E. Pree, “Large-area hexagonal silicon detectors for the CMS high granularity calorimeter,” *Journal of Instrumentation*, vol. 13, no. 02, p. C02022, 2018.
- [30] A. A. Maier, “Sensors for the CMS high granularity calorimeter,” *Journal of Instrumentation*, vol. 12, no. 06, p. C06030, 2017.
- [31] C.-F. Chien, C.-Y. Hsu, and K.-H. Chang, “Overall wafer effectiveness (OWE): a novel industry standard for semiconductor ecosystem as a whole,” *Computers & Industrial Engineering*, vol. 65, no. 1, pp. 117–127, 2013.
- [32] F. Prein and G. Allen, *Method of Maximizing Chip Yield for Semiconductor Wafers*, European Patent Application, Munchen, Denmark, 1998.
- [33] A. V. Ferris-Prabhu, “An algebraic expression to count the number of chips on a wafer,” *IEEE Circuits and Devices Magazine*, vol. 5, no. 1, pp. 37–39, 1989.
- [34] D. K. De Vries, “Investigation of gross die per wafer formulas,” *IEEE Transactions on Semiconductor Manufacturing*, vol. 18, no. 1, pp. 136–139, 2005.
- [35] C.-F. Chien, S.-C. Hsu, and C.-P. Chen, “An iterative cutting procedure for determining the optimal wafer exposure pattern,” *IEEE Transactions on Semiconductor Manufacturing*, vol. 12, no. 3, pp. 375–377, 1999.
- [36] C.-F. Chien, S.-C. Hsu, and J.-F. Deng, “A cutting algorithm for optimizing the wafer exposure pattern,” *IEEE Transactions on Semiconductor Manufacturing*, vol. 14, no. 2, pp. 157–162, 2001.
- [37] C.-S. Fan, “HIGH: a hexagon-based intelligent grouping approach in wireless sensor networks,” *Advances in Electrical and Computer Engineering*, vol. 16, no. 1, pp. 41–46, 2016.
- [38] J. H. Conway and R. K. Guy, *The Book of Numbers*, Copernicus, New York, NY, USA, 1996.
- [39] N. Hema and K. Kant, “Optimization of sensor deployment in WSN for precision irrigation using spatial arrangement of permanent crop,” in *Proceedings of the 2013 6th International Conference on Contemporary Computing, IC3 2013*, pp. 455–460, India, August 2013.
- [40] S. Kim, H. Cheon, S. Seo, S. Song, and S. Park, “A hexagon tessellation approach for the transmission energy efficiency in underwater wireless sensor networks,” *Journal of Information Processing Systems*, vol. 6, no. 1, pp. 53–66, 2010.
- [41] I. Litvinchev, L. Infante, and L. Ozuna, “Packing circular-like objects in a rectangular container,” *Journal of Computer and Systems Sciences International*, vol. 54, no. 2, pp. 259–267, 2015.
- [42] R. Torres-Escobar, J. A. Marmolejo-Saucedo, I. Litvinchev, and P. Vasant, “Monkey algorithm for packing circles with binary variables,” in *Advances in Intelligent Computing & Optimization*, vol. 866, pp. 547–559, Springer International Publishing, 2019.
- [43] A. Pankratov, T. Romanova, and I. Litvinchev, “Packing ellipses in an optimized rectangular container,” *Wireless Networks*, pp. 1–11, 2018.
- [44] S. I. Galiev and M. S. Lisafina, “Numerical optimization method for packing regular convex polygons,” *Computational Mathematics and Mathematical Physics*, vol. 56, no. 8, pp. 1402–1413, 2016.
- [45] T. Romanova, A. Pankratov, I. Litvinchev, Y. Pankratova, and I. Urniaieva, “Optimized packing clusters of objects in a rectangular container,” *Mathematical Problems in Engineering*, vol. 2019, Article ID 4136430, 12 pages, 2019.
- [46] I. Litvinchev, L. Infante, and E. L. O. Espinosa, *Using Valid Inequalities and Different Grids in LP-Based Heuristic for Packing Circular Objects*, vol. 9622 of *Lecture Notes in Computer Science*, 2016.
- [47] F. J. Kampas, I. Castillo, and J. D. Pintér, “Optimized ellipse packings in regular polygons,” *Optimization Letters*, 2019.
- [48] C. O. López and J. E. Beasley, “Packing unequal rectangles and squares in a fixed size circular container using formulation space search,” *Computers & Operations Research*, vol. 94, pp. 106–117, 2018.
- [49] C. O. López and J. E. Beasley, “Packing a fixed number of identical circles in a circular container with circular prohibited areas,” *Optimization Letters*, pp. 1–20, 2018.
- [50] F. J. Kampas, J. D. Pinter, and I. Castillo, “Packing Ovals in Optimized Regular Polygons,” *Optimization and Control*, 2019.
- [51] A. Pankratov, T. Romanova, and I. S. Litvinchev, “Packing ellipses in an optimized convex polygon,” *Journal of Global Optimization*, 2019.
- [52] P. Holub and J. Ryan, “Degree diameter problem on triangular networks,” *The Australasian Journal of Combinatorics*, vol. 63, no. 3, pp. 333–345, 2015.
- [53] B. Grünbaum and G. C. Shephard, “Tiling by regular polygons,” *Mathematics Magazine*, vol. 50, no. 5, pp. 227–247, 1977.
- [54] B. Grünbaum, J. C. P. Miller, and G. C. Shephard, “Uniform tilings with hollow tiles,” in *The Geometric Vein*, C. Davis, B. Grünbaum, and F. A. Sherk, Eds., pp. 17–64, Springer, New York, NY, USA, 1981.

